

# Hadronic blazar models and correlated X-ray/TeV flares

Jörg P. Rachen

*Sterrenkundig Instituut, Universiteit Utrecht, 3508 TA Utrecht, The Netherlands*

**Abstract.** The hypothesis that AGN jets might be the sources of the ultra-high energy cosmic rays has originally motivated the venture of TeV gamma ray astronomy. Surprisingly, after the discovery of TeV emission from blazars the attention has shifted to more traditional explanations which do not involve energetic hadrons, and there is even common belief that a hadronic interpretation is disfavored by observations. It is shown here that this is not the case, and that the currently observed spectra and variability features of blazars can be perfectly understood within hadronic blazar models. I also discuss how hadronic models might be observationally distinguished from common leptonic models, and point out some interesting aspects which could be relevant for the understanding of the differences between blazar classes.

## WHY HADRONIC MODELS?

### *AGN jets and the origin of cosmic rays*

Cosmic rays are observed up to the enormous energy of  $3 \times 10^{20}$  eV, and both theoretical and observational arguments suggest an extragalactic origin of these most energetic particles [1]. Since the cosmic ray arrival directions are largely randomized by Galactic and extragalactic magnetic fields, their sources cannot be easily identified from direct observations. However, if we assume that they gain their energy by acceleration (rather than by quantum processes, i.e., the decay of superheavy particles) their extreme maximum energy allows to derive quite restrictive selection criteria for possible acceleration sites. Most acceleration scenarios in astrophysics, for example Fermi acceleration [2], assume that particles are magnetically confined for some time  $t_{\text{acc}}$  in the accelerating region. This implies three fundamental constraints on the maximum proton energy,

$$E_{\text{cr}} < eBR\Gamma, \quad (1a)$$

$$E_{\text{cr}} < \frac{3}{2}m_p c^2 \Gamma (m_p/m_e) \sqrt{\eta B_c / \alpha_f B} \quad (1b)$$

$$E_{\text{cr}} < \eta e B \lambda_{\text{GZK}} \Gamma, \quad (1c)$$

which we call (a) the *confinement limit*, (b) the *synchrotron limit*, and (c) the *GZK limit*. The confinement limit simply expresses that the particle gyro-radius  $r_L$  in the magnetic field  $B$  is smaller than the system size  $R$ . The synchrotron limit expresses that  $t_{\text{acc}}$  is smaller than the synchrotron loss time, where  $B_c \approx 4 \times 10^{13}$  G is the critical magnetic

field, and  $\alpha_f \approx 1/137$  the fine structure constant. The parameter  $\eta = \Delta E/E$  is the fractional energy gain in a Larmor time,  $t_L = E/eBc$ , and one can show that for Fermi acceleration generally  $\eta < 1$  (see [3, App. D] for some discussion and references). The GZK limit expresses that proton acceleration must be faster than photohadronic losses at the microwave background, called the Greisen-Zatsepin-Kuzmin or GZK effect [4], and  $\lambda_{\text{GZK}} \sim 10$  Mpc is the appropriate attenuation length of protons with  $E > 10^{20}$  eV [5]. The GZK limit dominates over the confinement limit for sources on supercluster scales ( $\gtrsim 10$  Mpc), but it applies also to somewhat smaller scales (e.g. clusters of galaxies) since in such objects usually  $\eta \ll 1$  [6].

Only very few cosmic sources have been found which may satisfy all three conditions for  $E_{\text{cr}} \gtrsim 10^{20}$  eV, and all of them are connected to strong shocks in relativistic flows ( $\Gamma \sim 10\text{--}1000$ ): (a) the termination shocks of extended jets in radio galaxies [7], (b) compact jets in blazars [8,9], and (c) internal or external shocks in fireballs proposed to induce Gamma-Ray Bursts [10]. All of them are known as powerful emitters of non-thermal photons, in particular gamma rays. If we adopt the assumption that there is a universal ratio between cosmic ray and non-thermal photon emission (which is rather simplistic, but not unreasonable as an estimate), we could use their total contribution to the observed extragalactic gamma rays as a scale of their total power as cosmic ray sources. This clearly favors AGN over GRB, because AGN are known to produce 10–30% of all extragalactic gamma-rays (counting both resolved sources and diffuse background), while resolved GRB contribute less than 1%. Due to the GZK effect, another important selection criterion for UHECR sources is proximity. This disfavors powerful quasars, and also GRB if their cosmological distribution follows the star forming activity, since in both cases most power is emitted at large redshifts. In contrast, BL Lac objects and their proposed unbeamed counterpart, FR-I radio galaxies [11], seem to be more frequent in the current epoch than at large redshifts [12]. Since their jets may also satisfy the condition for the acceleration of UHECR, and they contribute significantly to the non-thermal radiation in the universe, blazars and FR-I radio galaxies may be regarded the primary candidates for the origin of the highest energy cosmic rays.

### *Hadronic vs. leptonic gamma-ray emission in blazars*

Energetic hadrons can lead to the emission of gamma rays via  $pp$  interactions with surrounding gas, or  $p\gamma$  interactions with ambient photons. This leads to the production of secondary  $e^\pm$  pairs, or mesons like  $\pi^\pm$  and  $\pi^0$ , which eventually decay into  $e^\pm$  pairs, photons and neutrinos. Electrons or pairs can produce high energy photons by synchrotron (or Compton) processes. The photons can either escape from the jet or produce new pairs in  $\gamma\gamma \rightarrow e^+e^-$  processes, which subsequently radiate a new generation of photons. In particular *synchrotron-pair cascades* of this kind are important if interactions of UHECR protons in AGN jets are considered, where they shift the energy in secondary radiation down from the extreme proton energies to the observable gamma-ray regime. This mechanism has been coined PIC for “proton induced cascades” [13].

The term “hadronic blazar models” is used for a large variety of models for the gamma-ray production in blazars, not all of which involve UHE cosmic rays. All in common is

just that they propose energetic protons as the main carrier of dissipated energy in the jet, rather than so-called “leptonic models”, which assume the bulk of the energy available for radiation in electrons or  $e^\pm$  pairs. Some hadronic models assume gamma-ray production in  $pp$  interactions invoked in the collision of jets with surrounding gas clouds, or in a very massive jet itself [14]. In a different class of models, protons have been suggested as being responsible just for the injection of energetic electrons, which then produce the observed photon emission by a synchrotron-self Compton (SSC) mechanism [15]. These models offer an interesting explanation for the observed strong variability in gamma-ray blazars due to intrinsic instabilities. They usually require only moderate proton energies, but very large densities of relativistic protons in the jet.

Following the motivation given above, I want to focus here on a different kind of hadronic models in which UHE cosmic rays in the jet interact with low energy target photons. They are split into two classes: (a) target photons are produced by synchrotron-radiating electrons co-accelerated with the protons [8], and (b) external target photons are present in the vicinity of the jet, as for example thermal photons emitted from an accretion disk or a warm dust torus [16]. In a realistic scenario, photons from both sources would be present. The local ratio of the external and internal photon energy density in a reference frame comoving with the jet differs hereby from the ratio of the observed external and internal luminosities by a factor  $\Gamma_{\text{jet}}^6$  (the corresponding number ratio of external to internal photons scales with  $\Gamma_{\text{jet}}^4$ ). It is therefore hard to constrain the local comoving density of external photons in the jet by observations. However, an indirect constraint on the external photon density has been pointed out by Protheroe and Biermann [17]: using a common accretion disk/torus model to estimate the radiation fields in AGN, they show that the emission of TeV photons would be strongly suppressed by  $\gamma\gamma$  absorption, if the emission region is close enough to the AGN that external photons could be relevant for  $p\gamma$  interactions. This is inconsistent with the observed spectra in TeV blazars like Mrk 501 or Mrk 421 (see below). Nevertheless, external photons can still be important in high luminosity EGRET blazars (like 3C 279) [9].

For the discussion of TeV blazars, we can therefore concentrate on so-called *synchrotron-self proton induced cascade* (SS-PIC) models, in which UHE protons interact with synchrotron photons emitted by electrons accelerated *in the same process* as the protons. One clear consequence of such models is that the gamma-ray emission due to the PIC process is in competition with SSC emission of the electrons. The relation of the luminosities of both processes is expressed by

$$\frac{L_{\text{PIC}}}{L_{\text{SSC}}} \lesssim 0.1 \frac{u_p(\hat{E}_p)}{u_{\text{ph}}} \left[ \frac{B}{1 \text{ G}} \right]^3 \left[ \frac{R}{10^{16} \text{ cm}} \right]^2, \quad (2)$$

where  $u_p = N_p^2 dN_p/dE_p$  is the energy density of protons at the maximum energy,  $\hat{E}_p$ , and  $u_{\text{ph}}$  is the bolometric energy density of the target photons (i.e., the *synchrotron* photons emitted by primary electrons), and  $B$  and  $R$  are magnetic field and size of the emission region, respectively. The relation gives in fact only an upper limit on the PIC contribution, since approximate equality assumes  $\hat{E}_p = eBR$ . We see that, if the UHE proton content of the jet is significant ( $u_p(\hat{E}_p) \geq u_{\text{ph}}$ ), and the maximum energy suffi-

cient to explain the observed UHECR ( $eB R \Gamma_{\text{jet}} \gtrsim 10^{20}$  eV, assuming a jet Lorentz factor  $\Gamma_{\text{jet}} \sim 10$ ), PIC emission will dominate over SSC at compact jet scales ( $R \lesssim 10^{16}$  cm) — and vice versa. For the likely case of adiabatic scaling of a dominantly transversal magnetic field with the jet radius,  $B \propto R^{-1}$ , the relative contribution of SSC emission would increase on larger scales. Therefore both processes may contribute to the observed radiation, although emission which is variable on short time scales (requiring small  $R$ ) would tend to be dominated by PIC. Defining clear signatures to distinguish PIC from SSC emission can therefore make the hypothesis that blazars and FR-I radio galaxies are the sources of UHE cosmic rays testable by GeV-TeV gamma-ray observations.

## SPECTRAL PROPERTIES OF SS-PIC MODELS

### *Synchrotron-pair cascades in power law target spectra*

At frequencies below the X-ray band, blazar spectra are well represented by broken power laws, in some cases even by single power laws down to the sub-mm regime [18]. These photons play a triple role in SS-PIC models: (i) they are targets for the initial  $p\gamma$  interactions, (ii) they are targets for the propagation of synchrotron pair cascades, and (iii) they allow clues on the particle spectrum of the primary accelerator. Let us, for simplicity, assume that the soft target photon number spectrum is described by a single power law,  $dN_{\text{ph}}/dE \propto E^{-\alpha_t-1}$ ,  $\alpha_t \sim 1$  is called the energy index of the target spectrum. The stationary electron spectrum producing these photons by synchrotron radiation must then have the form  $dN_e/dE \propto Q_{e,\text{acc}} t_{\text{syn}} \propto E^{-\alpha_e-1}$  with an energy index  $\alpha_e = 2\alpha_t$ , where  $Q_{\text{acc}} \propto E^{-\alpha_{\text{acc}}-1}$  is the number of electrons injected by the accelerator per unit time, and  $t_{\text{syn}} \propto E^{-1}$  is the synchrotron cooling time of the electrons. This means that the spectrum injected by the accelerator is a power law with energy index  $\alpha_{\text{acc}} = \alpha_e - 1$ . In contrast to electrons, cooling of protons is usually dominated by adiabatic [3] or advection losses [8]. Hence, the proton cooling time  $\bar{t}_p$  can be considered as energy independent, and the stationary proton spectrum is  $dN_p/dE \propto Q_{p,\text{acc}}(E)$ . If the accelerated protons have the same spectrum as the electrons, the proton power law energy index is  $\alpha_p \propto \alpha_{\text{acc}} = 2\alpha_t - 1$ , but we discuss also different choices of  $\alpha_p$ .

The opacity for the photohadronic production is  $\tau_{p\gamma} = \bar{t}_p/t_{p\gamma}$ , where  $t_{p\gamma} \propto E^{\alpha_t}$  is the according loss time scale. The major channel for hadronic gamma production is  $p\gamma \rightarrow \pi^0 + \dots$  with the subsequent decay  $\pi^0 \rightarrow \gamma\gamma$ . The resulting photons are dominantly absorbed by the soft target photons through  $\gamma\gamma$  pair production. The  $\gamma\gamma$  opacity has the same energy dependence as  $\tau_{p\gamma}$  for constant  $\bar{t}_p$ , that is  $\tau_{\gamma\gamma} \propto E^{-\alpha_t}$ , hence the stationary energy distribution of the primary photons from pion decay is  $dN_{\gamma}^{[0]}/dE = dN_p/dE (\tau_{\gamma\gamma}/\tau_{p\gamma}) \propto dN_p/dE$ . Saturated production of pairs in  $\gamma\gamma$  collisions (i.e.  $\tau_{\gamma\gamma} \gg 1$ ) then leads to [19]

$$\frac{dN_{\pm}^{[1]}}{dx} \propto \frac{1}{x^2} \int_{2x}^{\hat{x}_0} dx' \tau_{\gamma\gamma}(x') \frac{dN_{\gamma}^{[0]}}{dx'} \propto x^{-\alpha_{\pm}-1} = \begin{cases} x^{\alpha_t-\alpha_p-2} & \text{for } \alpha_p > \alpha_t \\ x^{-2} & \text{for } \alpha_p \leq \alpha_t \end{cases} \quad (3)$$

where  $x$  is the energy of photons or pairs in units of  $m_e c^2$ , and  $\hat{x}_0 = \hat{\gamma}_p m_{\pi}/2m_e \sim 100\hat{\gamma}_p$  is the maximum  $x$  of the primary injected photons. The pairs produce a new generation

of photons by synchrotron radiation, which are distributed in the stationary, saturated case as

$$\frac{dN_\gamma^{[1]}}{dx_1} \propto \frac{Q_{\text{syn}}^{[1]}(x_1)}{\tau_{\gamma\gamma}(x_1)} \propto x_1^{-\alpha_t-3/2} \left[ \frac{x^2 dN_\pm(x)}{dx} \right]_{x=x_1^{1/2}}, \quad (4)$$

i.e., as a power law with energy index  $\alpha_1 = \frac{1}{2}\alpha_\pm + \alpha_t$ .  $Q_{\text{syn}}^{[1]}(x) \propto x^{-\alpha_\pm/2}$  is the injected number of synchrotron photons per unit time at energy  $m_e c^2 x$  by the first generation of pairs. The stationary photons can inject a second generation of pairs, and so on. This *synchrotron-pair cascade* continues, and with each step the characteristic photon energy is reduced by

$$x_n \approx \frac{B}{4B_c} x_{n-1}^2 \quad \text{for} \quad Bx_{n-1} < 4B_c. \quad (5)$$

The latter condition expresses the classical limit of synchrotron radiation and is mostly fulfilled in hadronic blazar models; in the non-classical case the cascade propagates approximately as  $x_n = \frac{1}{2}x_{n-1}$ . Thus, the energy is rapidly reduced in each step once  $x \ll B_c/B \sim 10^{12}$ , and since  $\tau_{\gamma\gamma} \propto x^{\alpha_t}$  the opacity for the production of subsequent cascade generations quickly decreases. The cascade becomes unsaturated at a photon energy  $\sim m_e c^2 x_{\gamma\gamma}$ , defined by  $\tau_{\gamma\gamma}(x_{\gamma\gamma}) = 1$ , and dies out rapidly for  $x < x_{\gamma\gamma}$ . The photon spectrum emerging from the emitter is [19,13]

$$\frac{dN_{\gamma,\text{em}}}{dx} \propto \sum_{n=1}^{n^*+1} Q_{\text{syn}}^{[n]}(x) \left[ \frac{1 - e^{-\tau_{\gamma\gamma}(x)}}{\tau_{\gamma\gamma}(x)} \right] \propto \begin{cases} x^{\alpha_t - \alpha_1 - 1} & \text{for } x \ll x_{\gamma\gamma} \\ x^{-\alpha_1 - 1} & \text{for } x \gg x_{\gamma\gamma} \end{cases}, \quad (6)$$

where the sum extends over all cascade generations and  $n^*$  is the last generation with a highest photon energy  $\hat{x}_{n^*} > x_{\gamma\gamma}$  ( $\hat{x}_n$  is determined by repeated application of Eq. (5) on  $\hat{x}_0$ ). It can be shown that for typical blazar conditions  $n^* = 3-4$ , and that  $Q_{\text{syn}}^{[n^*]}$  dominates the emission around  $x_{\gamma\gamma}$  [20].

The term in brackets in Eq. (6) has the meaning of a mean escape probability of the photons from the emission region, and is strictly correct only for a plane-parallel geometry. However, the asymptotic behavior of the spectrum would be the same in any geometry, that is,  $x_{\gamma\gamma}$  marks a break in the spectrum by  $\Delta\alpha = \alpha_t$ , which we call the *opacity break*. This broken power law shape is typical for photospheric emission, which is in the nature of the SS-PIC models where the soft photons are responsible both for the production and absorption of gamma rays. It is directly observable unless there is significant absorption by external photons surrounding the jet, which would lead to an exponential cutoff  $\propto \exp(-\tau_{\gamma\gamma,\text{ext}})$ . The observed GeV–TeV spectra of TeV-blazars support in most cases a broken power law shape, as expected from the SS-PIC model for  $m_e c^2 x_{\gamma\gamma} \Gamma_{\text{jet}} \sim 1$  TeV, but are inconsistent with a rapid cutoff in this regime [18]. This has been used as an argument against external PIC models for TeV blazars [17]. An observed opacity break in the TeV regime is also expected from a direct determination of  $\tau_{\gamma\gamma}$  for typical blazar parameters [8], and from general considerations concerning the efficiency of hadronic blazar models [9].

## Robust features of hadronic blazar spectra

If we ignore the details of the cascade spectra in the vicinity of cutoffs or breaks, the spectral propagation can be described in terms of a simple algebra. If we call  $\alpha_n(x_n)$  the local spectral index in the vicinity  $x \sim x_n$ , we can introduce the relations

$$\alpha_n(x_n) = f_+[\alpha_{n-1}(x_{n-1})] \quad \text{for } x_n > x_{\gamma\gamma} \quad (7a)$$

$$\alpha_n(x_n) = f_-[\alpha_{n-1}(x_{n-1})] \quad \text{for } x_n < x_{\gamma\gamma} \quad (7b)$$

with

$$f_{\pm}[\alpha_n] = \max \left\{ \frac{1}{2}(\alpha_n \pm \alpha_t + 1), \frac{1}{2} \right\} \quad , \quad (7c)$$

where the dimensionless photon energy  $x_n$  propagates following Eq. (5). The spectrum of the  $k$ -th cascade is then given by  $f_+^k[\alpha_p]$  above the opacity break at  $x_{\gamma\gamma}$ , and by  $f_-[f_+^{k-1}[\alpha_p]]$  below (but above  $x'_{\gamma\gamma} = Bx_{\gamma\gamma}^2/4B_c \ll x_{\gamma\gamma}$ ), where  $f_+^k$  denotes the  $k$ -fold iterative application of  $f_+$ .

If we ask which cascade generation is dominant at a given energy we encounter a problem related to the energy propagation equation (5): for any given primary spectral feature at  $x_0$ , the position of its “image” in the  $n$ -th cascade is dependent on the magnetic field in the emitter by  $x_n \propto B^{2^n-1}$ . This means, for example, that the cutoff of the 4-th cascade generation is  $\hat{x}_4 \propto B^{15}$ , so that a variation of  $B$  by a factor of 2 over the emitting region would “smear out” the value of  $\hat{x}_4$  by more than 4 orders of magnitude. Fortunately, it is still possible to make some quite robust predictions on hadronic blazar spectra, since the cascade generation spectra converge quickly with  $k$  to  $f_+^\infty[\alpha_p] = 1 + \alpha_t$ , and  $f_-[f_+^\infty[\alpha_p]] = 1$ , independent of  $\alpha_p$ . Moreover, the power contained in each cascade generation is approximately equal for  $n < n^* + 1$  and rapidly decreases for larger  $n$ , so that the spectrum below  $x_{\gamma\gamma}$  is not strongly changed by adding generations with  $n > n^*$ . This allows the statement that *hadronic gamma-ray blazar spectra are described by a broken power law with energy indices  $\alpha \approx 1$  below, and  $\alpha \approx 1 + \alpha_t$  above a break observed at  $\sim 1$  TeV, where  $\alpha_t$  is the IR-X energy index of the source.*

So far we did not consider the cutoff in the target photon spectrum,  $\hat{x}_t$ , which is generally observed at an energy  $m_e c^2 \hat{x}_t \Gamma_{\text{jet}}$  between in the optical and X-ray regimes. We consider the target photon spectrum for  $x_t > \hat{x}_t$  as a power law with a steep energy index,  $\alpha'_t > \alpha_t + 1$ . Gamma rays with  $x_n < \hat{x}_t^{-1}$  then induce cascade photons below  $\tilde{x} = B/(4B_c \hat{x}_t^2)$  with an index  $\alpha'_{n+1} \approx f_-'[f_+^\infty[\alpha_p]] = \frac{1}{2}$ , where  $f_-'$  is the cascade operator defined in Eq. (7c) replacing  $\alpha_t$  with  $\alpha'_t$  (for  $\tilde{x} < x_{\gamma\gamma}$ ). Since this result is independent of the detailed value of  $\alpha'_t$  as long as  $\alpha'_t > \alpha_t + 1$ , we can consider it as valid for any steep cutoff, e.g., an exponential one. The energy  $m_e c^2 \tilde{x} \Gamma_{\text{jet}}$  marks a break in the spectrum, which is observable above the cutoff of the primary electron emission ( $\tilde{x} > \hat{x}_t$ ) if

$$\hat{\epsilon}_t = m_e c^2 \Gamma_{\text{jet}} \hat{x}_t \lesssim 100 \text{ eV} \left[ \frac{\Gamma_{\text{jet}}}{10} \right] \left[ \frac{B}{G} \right]^{1/3} . \quad (8)$$

For  $B < 100$  G this transition corresponds to the observationally motivated distinction between so-called low-energy-cutoff blazars (LBLs) and high-energy-cutoff blazars

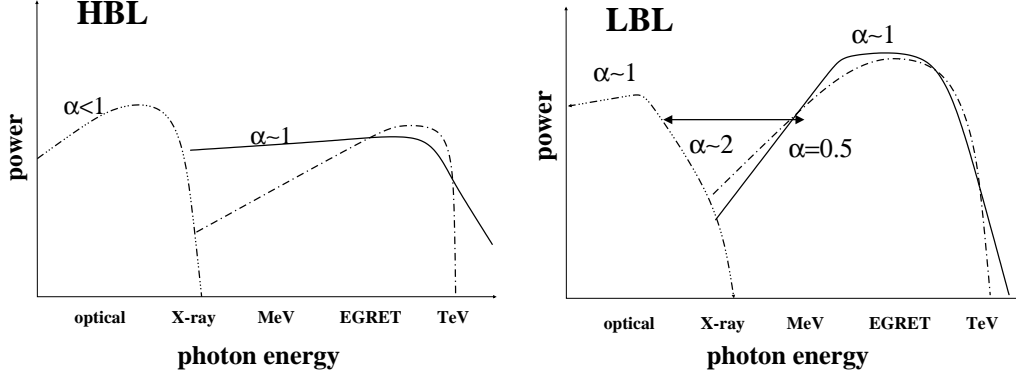


**FIGURE 1.** Generic SS-PIC spectra for HBL (left) and LBL (right) type blazars. Dashed high-energy lines show a typical spectral shape of an SSC model for comparison.

(HBLs) [11]. In the SS-PIC models we therefore expect fundamentally different shapes for the high energy spectra of these classes, as illustrated in Figure 1. Obviously, the spectrum for LBLs can easily be confused with an SSC spectrum, while a clear difference is predicted for HBLs in the MeV gamma-ray regime.

### *Narrow cascades: proton and muon synchrotron radiation*

Apart from  $\pi^0$  decay, energetic photons can also be produced by synchrotron radiation of the protons. Moreover, it has been shown that also the most energetic muons produced by the decay of photohadronically produced charged mesons can lose a significant fraction of their energy in synchrotron radiation in magnetic fields typical for SS-PIC blazar models, prior to their decay [3]. The total power ratio of synchrotron radiation compared to the  $\pi^0$  cascade injected by protons of the energy  $E_{\text{cr}}$  in the observer's frame is

$$\frac{L_{p,\text{syn}}}{L_{\pi^0}} \sim 4 \left[ \frac{E_{\text{cr}}}{10^{20} \text{ eV}} \right]^{1-\alpha_t} \left[ \frac{B}{10 \text{ G}} \right]^2 \left[ \frac{R}{10^{16} \text{ cm}} \right]^2 \left[ \frac{\Gamma_{\text{jet}}}{10} \right]^3 \left[ \frac{L_{\text{IR}}}{10^{44} \text{ erg/s}} \right]^{-1}, \quad (9)$$

where  $L_{\text{IR}}$  is the observed infrared luminosity of the blazar. For muon synchrotron radiation the ratio is  $L_{\mu,\text{syn}}/L_{\pi^0} \approx 2$  because of the photohadronic branching ratios [21].

If the jet contains cosmic ray protons up to an energy  $\hat{E}_{\text{cr}} \sim 3 \times 10^{20} \text{ eV}$  in the observer's frame,  $B \gtrsim 10 \text{ G}$  and the typical parameters assumed in Eq. (9) otherwise, proton synchrotron radiation extends up to observable energies of  $B \hat{x}_p^2 m_e^3 \Gamma_{\text{jet}} / (4 B_c m_p^3) \gtrsim 300 \text{ GeV}$ . Muon synchrotron radiation requires a minimal dimensionless energy  $x^* = E_\mu / m_e c^2 \Gamma_{\text{jet}} \sim 5 \times 10^{11}$  for  $B \sim 10 \text{ G}$  [3], and therefore extends from 30 GeV to 3 TeV using the same parameters. Since we have argued above that the opacity break is in the same regime, a significant fraction of this radiation can be reprocessed in a further cascade generation and would appear in the hard X-ray regime up to energies of  $\sim 10 \text{ keV}$  and  $\sim 100 \text{ keV}$  for reprocessed proton and muon synchrotron radiation, respectively.

The interesting aspect about these cascades becomes obvious when we consider their spectrum below the opacity break. Here, we assume for simplicity that proton syn-

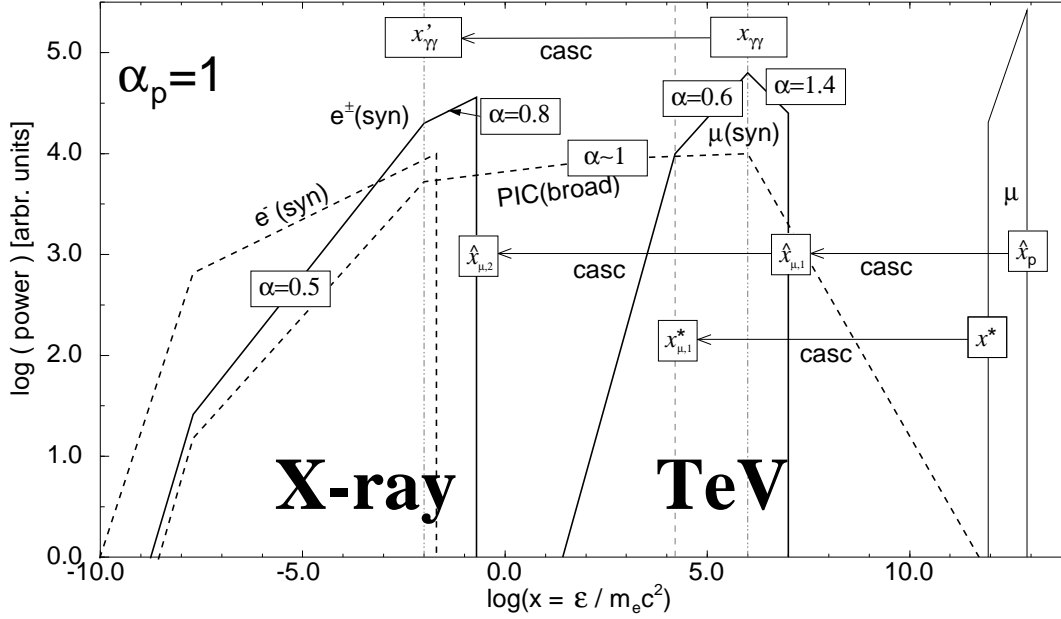


**FIGURE 2.** Schematic spectra of narrow cascades superposing the broad band emission of ordinary  $\pi^0$  cascades and primary electron synchrotron radiation — Spectral indices correspond to  $\mu$ -induced cascades for  $\alpha_p = 1$ , arrows indicate the cascading of spectral features. The proton-synchrotron cascade is omitted for clarity, but has a similar structure at photon energies about a factor of 10 lower (see also [23]).

chrotron radiation is significant, but not dominant over adiabatic or advection losses. In this case, the proton synchrotron spectrum has an energy index  $\alpha_{p,1} = \frac{1}{2}\alpha_p \sim 0.5$ . For muons synchrotron cooling is always dominant (otherwise it is suppressed due to muon decay), and we obtain  $\alpha_{\mu,1} = f^-[\alpha_p] \sim 0.5$  for  $x_{\gamma\gamma} > x > x_1^* = Bx^*{}^2 m_e^3 / (4B_c m_\mu^3)$ , and  $\alpha_{\mu,1} = -\frac{1}{3}$  below from synchrotron emission below the characteristic frequency. Hence, both processes produce spectra very much flatter than those arising from ordinary,  $\pi^0$  induced cascades. Above the opacity break, the spectra steepen by  $\alpha_t \sim 1$ , which means that the peak of the luminosity is reached at the opacity break. Here, the dominance of this component over the broad  $\pi^0$  cascades is even stronger than expected from the power ratio factors derived above, since it is first generation synchrotron emission, while the  $\pi^0$  emission from the same protons is broadened through the cascading process. The spectral indices expected from the narrow cascades below and above the opacity break (Fig. 2) are consistent with the typical EGRET and TeV indices, respectively, observed in Mrk 421 and Mrk 501 [18]. The spectral indices of the second cascade are obtained from a second application of the operator  $f^-$ , yielding again values around 0.5 steepening by  $\frac{1}{2}\alpha_t$  above an X-ray break observable at  $m_e c^2 \Gamma_{\text{jet}} x'_{\gamma\gamma}$  with  $x'_{\gamma\gamma} \approx Bx_{\gamma\gamma}^2 / 4B_c$  (see Fig. 2). These compare well to the indices observed by Beppo-SAX in three prominent flares of Mrk 501 in April 1997 [22]. The luminosity in the X-ray peak depends sensitively on the energy of the opacity break, which determines how much energy of the TeV peak is reprocessed. For example, in the SS-PIC model by Mücke and Protheroe [23] the opacity break is at  $m_e c^2 x_{\gamma\gamma} \Gamma_{\text{jet}} \sim 25$  TeV, which explains why their X-ray peak from



reprocessed proton synchrotron radiation is strongly suppressed. For suitable parameters, however, *narrow PIC emission can produce a two-bump spectrum with comparable peaks the TeV and the X-ray regime*, as illustrated in Figure 2.

## VARIABILITY AND CORRELATED FLARES

### *Flares and the quiescent background*

A major result of the simultaneous multiwaveband observations of Mrk 421 and Mrk 501 was that their variability in the X-ray and TeV-regime is largely correlated, and stronger than in other wavebands. This has been used as an argument against a hadronic interpretation of their gamma-ray emission, since ordinary cascade models expect a quite model independent spectral index (as explained above), which implies that the gamma-ray variability of such sources should be comparable at all gamma-ray energies.

Obviously, this picture changes if we consider narrow cascades. In order to play a dominant role in the emission, these require conditions which allow to produce cosmic rays of extremely high energies. Let us assume now that such conditions are not always present in the jet, but only in some confined regions for a limited time. Of course, we may still assume that also in other regions the jet accelerates protons and electrons, albeit not to such high energies. This would lead to a permanent “glow” of the jet, which is dominated by the emission of primary electrons and  $\pi^0$  induced cascades with a spectrum comparable to the case illustrated in Fig. 1 for HBLs, which is consistent with observations of the quiescent emission of Mrk 421. A short flare which contains UHE protons able to produce narrow cascades, and which is energetic enough to compete with the total emission of the rest of the jet, would then cause the strongest variability in the energy regimes where the flare spectrum peaks, and these are the X-ray and TeV regimes. At other wavebands, the variability may be low, or not present at all since the emission there may continue to be dominated by the quiescent background (see Fig. 3).

### *Opacity and variability*

The assumption of the existence of an opacity break in or below the TeV regime is vital for a successful explanation of blazar spectra in an SS-PIC model. This has some very interesting implications if the emission is variable. Let us assume a nearly plane-parallel geometry of length  $R$  for a region emitting photons simultaneously over its entire volume, over a time scale  $t_{\text{rad}} \ll R/c$ . In the optically thin case, this would induce a flare of duration  $R/c$  owing to the run-time differences of photons. If the emitter is opaque at some energy  $x$ , i.e.,  $\tau_{\gamma\gamma}(x) \gg 1$ , only photons emitted within a distance  $R/\tau_{\gamma\gamma}$  can reach the observer, causing a flare of duration  $R/c\tau_{\gamma\gamma}$ .

Applying this to SS-PIC models with an opacity break below TeV, we would therefore expect that the observed multi-TeV variability becomes systematically faster with increasing photon energy, while the variability time scales are energy independent at X-ray or EGRET energies that are below the opacity break. Of course, the simple relation  $T_{\text{var}} = T_{\text{var},0}/\tau_{\gamma\gamma}$  for  $\tau_{\gamma\gamma} > 1$ , and  $T_{\text{var}} = T_{\text{var},0}$  for  $\tau_{\gamma\gamma} < 1$  is unlikely to apply

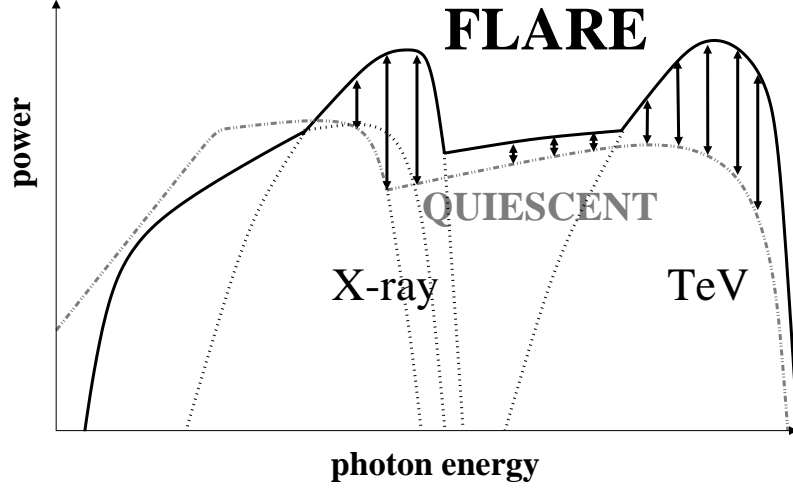


**FIGURE 3.** Correlated variability on blazars as a result of flaring, narrow PIC emission superposing a non-peaked background from the surrounding jet.

to SS-PIC, since both cascade injection and propagation involves time scales  $\sim R/c$ . Nonetheless, the effect remains qualitatively in the sense that it reduces the variability time from  $\sim t_{\text{rad}} + R/c$  to  $\sim t_{\text{rad}}$  for  $\tau_{\gamma\gamma} \gg 1$ . This may explain some recent simultaneous X-ray/TeV observations of Mrk 501 which indicate a TeV variability about a factor of 3 shorter than at three different X-ray energies, which all show the same time curve [18]. In contrast, optically thin SSC models would expect that there is some X-ray energy which shows the same variability as observed in the TeV.

## SUPPLEMENTARY ASPECTS

### *Particle acceleration in the SS-PIC model*

Some of the properties of the SS-PIC model discussed above on a purely heuristical base (i.e., the assumption that UHECR are produced) can be put on a more rigid foundation if we include the acceleration process. For jets the most reasonable assumption is Fermi acceleration at shocks or plasma turbulence [2]. If a particle with mass  $m$  is accelerated on a time scale  $t_{\text{acc}} = \eta^{-1} t_L$ , where  $\eta$  has the same meaning as in Eqs. (1), then the cutoff of the synchrotron radiation emitted by the particle satisfies the condition

$$\hat{\epsilon} \lesssim \pi \eta m c^2 / \alpha_f \sim 400 \eta m c^2, \quad (10)$$

which is reached if the particle energy limited by synchrotron cooling ( $t_{\text{acc}} = t_{\text{syn}}$ ). Applying Eq. (10) to synchrotron radiating protons we find a maximum observed photon energy of  $\approx [4 \text{ TeV}] \eta_p$  (assuming  $\Gamma_{\text{jet}} \sim 10$ ). For Fermi acceleration we can write  $\eta(E) \sim [\beta \delta B(r_L)/B]^2$ , where  $\beta$  is the velocity of the shock or plasma wave, and  $\delta B(r_L)/B$  is the fractional magnetic field turbulence on the scale of the particle gyro-radius,  $r_L = E/eB$  (see [3, App.D], and references therein). Obviously, in order

to explain photons observed above 300 GeV by proton synchrotron radiation we need  $\eta(\hat{E}_{\text{cr}}) > 0.1$ , which requires relativistic shocks and strong turbulence on the largest scales in the system. In this picture, correlated flares in blazars are due to the appearance of transient relativistic shocks in a turbulent flow, while the background emission is due to continuous acceleration at omnipresent weak shocks or plasma turbulence.

Applying Eq. (10) to accelerated electrons, we find a maximum synchrotron photon energy of  $\approx [2 \text{ GeV}] \eta_e$  for  $\Gamma_{\text{jet}} \sim 10$ , which implies  $\eta_e \sim 10^{-9} - 10^{-5}$  to explain the observed IR-X cutoffs in blazars. The large difference between  $\eta_p$  and  $\eta_e$  can be understood from the theory of plasma turbulence, noting that the electrons probe very much smaller scales of the turbulence than the protons. If the turbulence is described by  $\eta(E) \propto [\delta B(r_L)/B]^2 \propto E^y$ , we find

$$\hat{\epsilon}_{e,\text{syn}} \sim \hat{\epsilon}_{p,\text{syn}} \left[ m_e/m_p \right]^{(3y+2)/(2-y)}, \quad (11)$$

which is obviously independent of Doppler boosting. Biermann and Strittmatter [24] pointed out that the near infrared cutoffs observed in many quasars (e.g., LBLs) can be understood if they accelerate protons to the GZK limit, and the plasma turbulence is described by a Kolmogorov spectrum ( $y = \frac{2}{3}$ ). In terms of Eq. (11), we would obtain  $\hat{\epsilon}_{e,\text{syn}} \sim 1 \text{ eV}$  for  $y = \frac{2}{3}$  and  $\hat{\epsilon}_{p,\text{syn}} = 10 \text{ GeV}$ , which is consistent with the observations of LBLs and would imply  $\eta_p \sim 10^{-3}$ . The Kolmogorov spectrum applies to fully developed hydrodynamical turbulence if the magnetic field does not significantly contribute to the total energy density of the fluid. In a magnetically dominated plasma a Kraichnan turbulence spectrum would be expected [24], that is  $y = \frac{1}{2}$ . Combining this with  $\hat{\epsilon}_{p,\text{syn}} \sim 300 \text{ GeV}$  which we required for blazars with correlated X-ray/TeV variability, we find  $\hat{\epsilon}_{e,\text{syn}} \sim 10 \text{ keV}$ , which corresponds to X-ray cutoffs typically observed in HBLs (note that the flare emission up to  $>100 \text{ keV}$  in Mrk 501 is explained by hadronic cascades in this model). This allows an interesting explanation of the physical difference between these blazar classes: while LBL jets are energetically dominated by the hydrodynamic motion of the plasma, and involve only non-relativistic shocks and/or weak to moderate turbulence, HBL jets are strongly turbulent, magnetically dominated flows, in which also relativistic shocks occur. More aspects of particle acceleration in the SS-PIC model are discussed in [23].

### *Gamma rays, cosmic rays and neutrinos*

One prediction which is unique to hadronic blazar models is the production of energetic neutrinos with a luminosity comparable to gamma-rays. The detection of such neutrinos, in particular if correlated with blazar flares, would thus be a “smoking gun” for the hadronic scenario; unfortunately, the neutrino fluxes from single blazar flares are that low that this can hardly be expected within the next decades [3]. However, we would expect to find *diffuse* VHE neutrino fluxes comparable to the the diffuse extragalactic gamma ray background (DEGRB), if a considerable fraction of the extragalactic gamma rays are of hadronic origin. This would also imply that a significant fraction of the UHECR flux is produced by the same process [9]. To utilize these relations to decide

the nature of gamma-ray emission in blazars, we need to determine which fraction to the DEGRB they contribute — which is again a task for gamma-ray astronomy.

In conclusion, although VHE neutrino observations will be very important to clarify the origin of cosmic rays, I still see the currently better technical possibilities to decide this question on the side of gamma-ray astronomy. To do this by revealing the nature of gamma-ray emission from blazars will require (i) a complete coverage of the gamma-ray wavebands from MeV to multi-TeV energies with sufficient spectral resolution, together with more campaigns allowing truly simultaneous multifrequency monitoring, and (ii) a comprehensive discussion of the data in the view of possible leptonic *and* hadronic explanations.

**Acknowledgments.** I wish to thank A. Achterberg, A. Atoyan, R. Bingham, J. Kirk, K. Mannheim, A. Mastichiadis, A. Mücke, and R. Sambruna for interesting and helpful discussions, and the LOC for support allowing me to visit the meeting. This work was supported in part by the EU-TMR network Astro-Plasma Physics, under contract number ERBFMRX-CT98-0168.

## REFERENCES

1. P. L. Biermann, J. Phys. G **23**, 1 (1997), and references therein.
2. L. O'C. Drury, Rep. Prog. Phys. **46**, 973 (1983), and references therein.
3. J. P. Rachen and P. Mészáros, Phys. Rev. D **58**, 123005 (1998).
4. K. Greisen, Phys. Rev. Lett. **16**, 748; G. Zatsepin and V. Kuzmin, JETP Lett. **4**, 78 (1966).
5. F. W. Stecker, Phys. Rev. Lett. **21**, 1016 (1968).
6. C. A. Norman *et al.*, ApJ **454**, 60 (1995); H. Kang *et al.*, MNRAS **286**, 257 (1997).
7. J. P. Rachen and P. L. Biermann, A&A **272**, 161 (1993).
8. K. Mannheim, A&A **269**, 67 (1993); Space Sci. Rev. **75**, 331 (1996).
9. K. Mannheim *et al.*, Phys. Rev. D submitted, astro-ph/9812398.
10. M. Vietri, ApJ **453**, 883; E. Waxman, Phys. Rev. Lett. **75**, 386 (1995).
11. C. M. Urry and P. Padovani, PASP **107**, 803 (1995).
12. N. Bade *et al.*, A&A **334**, 459 (1998).
13. K. Mannheim *et al.*, A&A **251**, 723 (1991).
14. A. Dar and A. Laor, ApJ **478**, L5 (1997); M. Pohl, these proceedings.
15. J. G. Kirk and A. Mastichiadis, Nature **360**, 135 (1992); D. Kazanas and A. Mastichiadis, ApJ **518**, L17 (1999).
16. R. Protheroe, in *Accretion Phenomena and Related Outflows*, ed. D. Wickramasinghe *et al.*, IAU Colloquium 163, p. 585 (1997).
17. R. Protheroe and P. L. Biermann, Astropart. Phys. **6**, 293 (1997).
18. R. Sambruna, these proceedings, and references therein.
19. R. Svensson, MNRAS **227**, 403 (1987).
20. K. Mannheim, Phys. Rev. D **48**, 2408 (1993).
21. A. Mücke *et al.*, Proc. 19th Texas Symposium, Paris, 1998, astro-ph/9905153.
22. E. Pian *et al.*, ApJ **497**, L17 (1998).
23. A. Mücke and R. Protheroe, these proceedings, and private communication.
24. P. L. Biermann and P. A. Strittmatter, ApJ **322**, 643 (1987), and references therein.